

**INVESTIGATING SKELETAL MUSCLE ADAPTATIONS
DUE TO BTX-A INJECTIONS USING AGENT-BASED
MODELLING**

by

Mohammed H. M. Hammouda

B.S., in Mechanical Engineering, Texas A&M University at Qatar, 2015

Submitted to the Institute of Biomedical Engineering

in partial fulfillment of the requirements

for the degree of

Master of Science

in

Biomedical Engineering

Boğaziçi University

2020

**INVESTIGATING SKELETAL MUSCLE ADAPTATIONS
DUE TO BTX-A INJECTIONS USING AGENT-BASED
MODELLING**

APPROVED BY:

Prof. Dr. Can A. Yücesoy
(Thesis Advisor)

Doç. Dr. Gönenç Yücel

Doç. Dr. Yunus Ziya Arslan

DATE OF APPROVAL: 10 February 2020

ACKNOWLEDGMENTS

To everyone who helped me start and finish this thesis especially Dr. Can A. Yücesoy and my amazing family.



ACADEMIC ETHICS AND INTEGRITY STATEMENT

I, Mohammed H. M. Hammouda, hereby certify that I am aware of the Academic Ethics and Integrity Policy issued by the Council of Higher Education (YÖK) and I fully acknowledge all the consequences due to its violation by plagiarism or any other way.

Name :

Signature:

Date:

ABSTRACT

INVESTIGATING SKELETAL MUSCLE ADAPTATIONS DUE TO BTX-A INJECTIONS USING AGENT-BASED MODELLING

Local application of Botulinum Toxin Type-A (BTX-A) has been the gold standard for spasticity management in children with Cerebral Palsy. The treatment aims to reduce the passive resistance of force at the joint and increase the joint range of motion. However, recent studies have reported results contradictory to treatment aims including increased passive force, increased muscle stiffness and decreased length range of force exertion which have been attributed to the increased collagen content in the muscle Extracellular Matrix (ECM) confirmed by histological findings. Moreover, a recent finite element analysis study has reported that BTX-A injections were found to increase the injected muscle fibers' strain. Hence, to understand these muscle adaptations and the effects of strain on muscle structure and function, the Agent-Based Modelling (ABM) method was used. The advantages of this method over other methods is that it allows studying muscle adaptations at the cellular level with the complex interactions modelled. This study was modelled in three cases comparing the BTX-A model, BTX-A-Free model and a middle half paralyzed (MHP) model similar to that used in the recent finite element model. Two of the cases compared the BTX-A-Free fascicle against the BTX-A and the MHP fascicles and the third case compared the BTX-A-Free case to a modified MHP case which included the reported BTX-A induced atrophy and the decaying effects of BTX-A 7-10 days after injection. The collagen increase in the cases was approximately 33%, 33%, and 20.3% respectively. This study revealed that although the BTX-A induced strain increase was found to increase collagen content of the ECM, other important factors such as the BTX-A induced atrophy may also play a significant role in collagen increase in the muscle ECM.

Keywords: Botulinum Toxin Type-A, Skeletal Muscle Adaptations, Cerebral Palsy, Agent-based Modelling.

ÖZET

BOTULINUM TOXIN TYPE-A SEBEP OLDUĞU ISKELET KASI ADAPTASYONLARININ AJAN TABANLI MODELLEME İLE ARAŞTIRILMASI

Botulinum Toksin Tip-A'nın (BTX-A) lokal uygulaması, Serebral Palsili çocuklarda spastisite yönetimi için altın standart olmuştur. Tedavi eklemdeki kuvvetin pasif direncini azaltmayı ve eklem hareket aralığını artırmayı amaçlamaktadır. Bununla birlikte, son çalışmalar, histolojik bulgularla doğrulanan kas Ekstrasellüler Matrisinde (ECM) artmış kollajen içeriğine atfedilen artan pasif kuvvet, artan kas sertliği ve azaltılmış kuvvet efor aralığı dahil olmak üzere tedavi amaçlarıyla çelişen sonuçlar bildirmiştir. Buna ek olarak, son zamanlarda yapılan bir sonlu elemanlar analizi çalışması, BTX-A enjeksiyonlarının enjekte edilen kas liflerinin kasılması arttırdığı bulunmuştur. Bu nedenle bu kas adaptasyonlarını ve gerginliği kas yapısı ve fonksiyonu üzerindeki etkilerini anlamak için Ajan Tabanlı Modelleme (ABM) yöntemi kullanılmıştır. ABM yönteminin diğer yöntemlere göre avantajları, modellenen karmaşık etkileşimlerle hücresel düzeyde kas adaptasyonlarının incelenmesine izin vermesidir. Bu çalışma BTX-A modelini, BTX-A-Free modelini ve son sonlu eleman modelinde kullanılan benzer bir orta yarı felçli (MHP) modelini karşılaştıran üç durumda modellenmiştir. Olgulardan ikisi BTX-A-Free fasikülü BTX-A ve MHP fasiküllerine karşı karşılaştırdı ve üçüncü vaka BTX-A-Free vakasını bildirilen BTX-A ile indüklenen atrofiyi ve bozulmayı içeren modifiye edilmiş bir MHP vakası ile karşılaştırdı BTX-A'nın enjeksiyondan 7-10 gün sonra etkileri. Olgulardaki kollajen artışı sırasıyla yaklaşık %33, %33 ve %20.3 idi. Bu çalışma, kasılmaya sebep olan BTX-A'nın ECM'nin kollajen miktarını arttırdığı bulunmasına rağmen, BTX-A ile indüklenen atrofi gibi diğer önemli faktörlerin de kas ECM'sinde kollajen artışında kollajen artışında önemli bir rol oynayabileceğini ortaya koymuştur.

Anahtar Sözcükler: Botulinum Toksini Tip-A, İskelet Kası Adaptasyonları, Serebral Palsi, Ajan Tabanlı Modelleme.

TABLE OF CONTENTS

ACKNOWLEDGMENTS	iii
ACADEMIC ETHICS AND INTEGRITY STATEMENT	iv
ABSTRACT	v
ÖZET	vi
LIST OF FIGURES	ix
LIST OF ABBREVIATIONS	xii
1. INTRODUCTION	1
1.1 Skeletal Muscle Structure	1
1.1.1 The Main Components of The Skeletal Muscle	1
1.1.1.1 Muscle Fibers	1
1.1.1.2 The Extracellular Matrix (ECM)	3
1.1.1.3 Fibroblasts	4
1.1.1.4 Chemokines	6
1.2 Skeletal Muscle Pathology And Cerebral Palsy (CP)	8
1.2.1 Using Botulinum Toxin Type-A in the Treatment of CP	9
1.2.2 Recent Investigations on BTX-A Effects on Muscle Mechanics.	10
1.3 The Agent-Based Modelling Method	15
1.4 Goal of the Study	18
2. METHODS	19
2.1 The AB Model	19
2.1.1 Components of the AB Model	19
2.1.2 Equations Governing the Model	22
2.2 The Modelled Cases	23
2.2.1 Case 1 BTX-A Vs. BTX-A-Free	23
2.2.2 Case 2 MHP Vs. BTX-A-Free	23
2.2.3 Case 3 BTX-A-Free Vs. Physiological MHP	24
2.3 Modelling Procedures	24
2.4 Simulation Settings	25
2.5 Processing of Data and Statistics	25

3. RESULTS 27

 3.1 Case 1: BTX-A Vs. BTX-A-Free 27

 3.2 Case 2: MHP Vs. BTX-A-Free 27

 3.3 Case 3: BTX-A-Free Vs. Physiological MHP 28

 3.4 Validation 29

4. DISCUSSION 31

5. CONCLUSION 35

REFERENCES 36



LIST OF FIGURES

Figure 1.1	Illustration showing the hierarchy of the skeletal muscle structure [1].	1
Figure 1.2	Illustration inspired from the work of A. F. Huxley and R. Niedergerke showing the proposed sliding filament theory and the structure of the sarcomeres in both the relaxed and contracted states (Slightly modified from Scitable [2]).	2
Figure 1.3	The length-force relationship curve of the sarcomere's force production capacity compared to its length [3].	2
Figure 1.4	Human Cardiac Fibroblasts (CAF) showing the cell body in green and the nucleus in blue. Immunostaining for Vimentin, 600x [4].	4
Figure 1.5	BTX-A blocking of Acetylcholine (ACh) at the presynaptic cleft at the neuromuscular junction [5].	10
Figure 1.6	An increase in the passive forces of both the EDL and EHL after both proximal and distal lengthening can be seen by looking at the BTX-A passive force markers (grey squares) [6].	11
Figure 1.7	An increase in the passive forces of both the EDL and EHL after both proximal and distal lengthening can be seen by looking at the BTX-A passive force markers (grey squares) [6].	11
Figure 1.8	Histological samples of the anterior crucial muscle stained for Gomori trichrome for connective tissue. From the left tibialis anterior (TA), extensor hallucis longus (EHL) and extensor digitorum longus (EDL) control (upper) muscles were compared to BTX-A (lower) treated muscles [6].	12

Figure 1.9	The finite element model of the EDL muscle showing three muscle elements in series and seventeen in parallel. Each combination of three muscle elements arranged in series constructs a whole fascicle, seventeen in total. The proximal and distal ends of the muscle elements are connected to elements representing the muscle aponeuroses [7].	13
Figure 1.10	Deformed muscle's shape after distal lengthening of BTX-A treated muscle modelled by paralyzing the proximal half (PHP), middle half (MHP), or distal half (DHP) of the muscle.	13
Figure 1.11	The effects of modelling the partial paralysis cases of the BTX-A case on muscle fiber direction mean strain. $\hat{\mu}_m$, or muscle lengths are shown above each figure. The dark plots with the dark bullets indicate the active muscle parts while the grey plots and bullets indicate the paralyzed ones [7].	14
Figure 1.12	Finite element analysis results show increased strain in the BTX-A muscle fiber versus the control muscle fiber [7].	15
Figure 1.13	The main components of an agent-based model [8].	16
Figure 2.1	The AB generated muscle fascicle cross section showing the main components; muscle fibers (red), ECM (grey), fibroblasts(yellow) and chemokines (not shown). The AB model was developed using the Netlogo 6.0.4 software [9].	20
Figure 2.2	The inputs and outputs of the main components of the model.	21
Figure 2.3	The left fascicle shows the patches where the BTX-A strain was applied whereas the right fascicle shows where the BTX-A-Free strain was applied.	23
Figure 2.4	The left fascicle shows the patches where the BTX-A strain was applied whereas the right fascicle shows where the BTX-A-Free strain was applied.	24
Figure 2.5	Graph showing the averages of collagen turnover and the gradual stabilization after approximately 50 runs for the three fascicles with different strain conditions.	25

Figure 3.1	The collagen sum, collagen density, collagen turnover and fibroblast count for the fascicle of case 1.	27
Figure 3.2	The collagen sum, collagen density, collagen turnover and fibroblast count for the fascicle of case 2.	28
Figure 3.3	The collagen sum, collagen density, collagen turnover and fibroblast count for the fascicle of case 3.	29
Figure 3.4	The effects of multiplying the BTX-A strain by a factor of 100 on the collagen sum, collagen density, collagen turnover and fibroblast activity.	29
Figure 4.1	Histological comparison between the control BTX-A injected and contralateral muscles after 1, 3, and 6 months of BTX-A injection [10].	34

LIST OF ABBREVIATIONS

ABM	Agent-Based Modelling
BTX-A	Botulinum Toxin Type-A
CP	Cerebral Palsy
CSA	Cross-Sectional Area
ECM	Extracellular Matrix
IL-1	Interleukin-1
IGF-1	Insulin-like Growth Factor-1
MHP	Middle Half Paralyzed
PDGF	Platelet-Derived Growth Factor
TGF- β	Transforming Growth Factor-Beta

1. INTRODUCTION

1.1 Skeletal Muscle Structure

The hierarchical structure of skeletal muscle is shown in Figure 1.1. Numerous myofibrils are contained within a muscle fiber. The muscle fibers are the cells of the skeletal muscle tissue and the extracellular matrix (ECM) within and around the muscle is comprised of connective tissue layers including sarcolemma (cell membrane), basal lamina, endomysium, perimysium and epimysium. Each muscle fiber is surrounded by a tubular connective tissue structure referred to as the endomysium. Groups of muscle fibers are bundled together into fascicles, and each fascicle is surrounded by another layer of the ECM, called the perimysium. In addition to that, the whole muscle group and muscle subgroups are covered by the epimysium. In a transverse view of muscle, one can observe the arrangement of muscle fibers and the ECM. With the help of staining techniques other aspects of fibers and muscle structure can be identified, such as the fiber type, nucleus placement, satellite stem cells, fibroblasts, blood vessels and nerves [1].

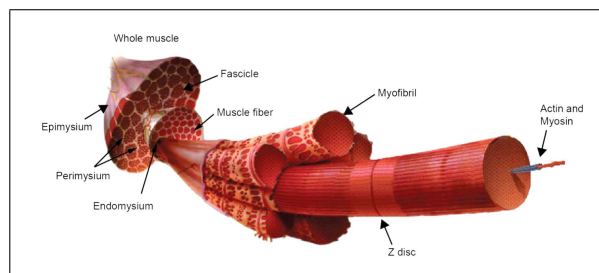


Figure 1.1 Illustration showing the hierarchy of the skeletal muscle structure [1].

1.1.1 The Main Components of The Skeletal Muscle

1.1.1.1 Muscle Fibers. Muscle fibers are typically large cells, some 20-100 in diameter and many centimeters long, up to 12 cm. They are multinucleated cells and with their nuclei typically more concentrated near the neuromuscular junction.

The most obvious property of muscle fibers is their striated pattern due to the highly organized and patterned A and I bands [11]. These bands, shown in Figure 1.2 play a very important role in the currently used model of muscle contraction known as the sliding filament theory. The theory, first proposed in 1954 by A. F. Huxley and R. Niedergerke and H. E. Huxley and J. Hanson, explains that the stationary myosin protein found in the A band binds to and contracts the actin protein found in the I band causing the muscles sarcomeres to shorten which initiates muscle contraction [12].

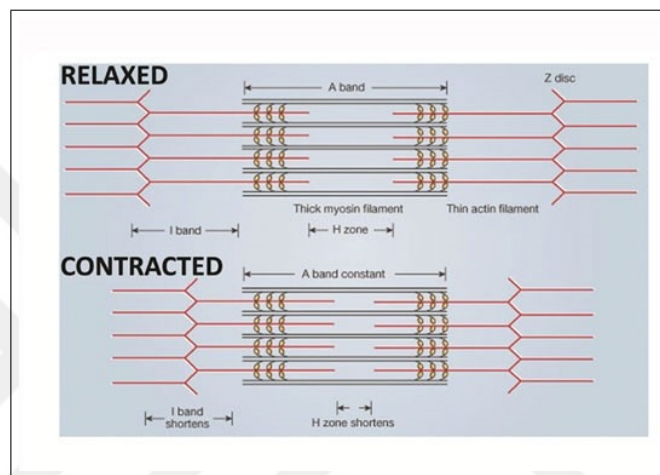


Figure 1.2 Illustration inspired from the work of A. F. Huxley and R. Niedergerke showing the proposed sliding filament theory and the structure of the sarcomeres in both the relaxed and contracted states (Slightly modified from Scitable [2]).

As the actin slides on the myosin protein chain, the sarcomere shortens, and force is produced in the muscle fibers according to the length-force relationship shown in Figure 1.3.

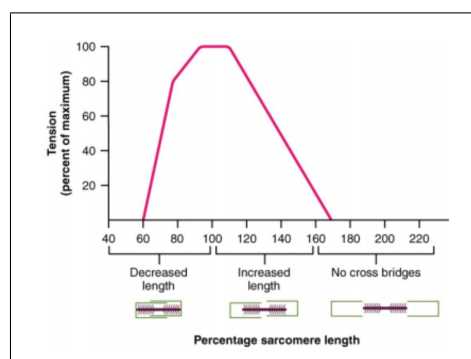


Figure 1.3 The length-force relationship curve of the sarcomere's force production capacity compared to its length [3].

As the length decreases in the muscle's sarcomeres due to the actin contraction, a higher tension force is generated in the muscle. This continues as the muscle tension reaches a maximum followed by a constant force production where the muscle can not produce more force due to the engagement of all the cross bridges or the actin-myosin binding sites. However, as the muscle sarcomeres increase in length, the number of cross bridges lessens and hence less force is produced. This decrease in force continues until force production stops when there are no cross-bridges taking place [13].

This relationship helps in understanding the muscle's mechanism of work at the smallest level.

Moreover, it is important to know that muscle fibers are classified into four types according to their contractile and metabolic properties as the following: type I, type IIa, type IIb, and type IIx [1]. Contractile properties refer to the muscle fiber's speed of contraction and relaxation, and the specific force it can produce. On the other hand, metabolic properties refer to whether aerobic or anaerobic pathways are used to produce energy in the form of ATP from fuels [11]. The twitch speeds of the muscle types arranged from fastest to slowest are as the following: type IIb > type IIx > type IIa > type I [1].

1.1.1.2 The Extracellular Matrix (ECM). The extracellular matrix is a highly dynamic three-dimensional noncellular matrix composed of collagen, proteoglycans/ glycosaminoglycans, elastin, fibronectin, laminins, and several other glycoproteins forming a complex network where cells reside. The extracellular matrix is found in all organs and it undergoes continuous remodelling to maintain cell normal homeostasis. In addition to providing a scaffold for cells, the extracellular matrix also mediates cellular processes such as growth, adhesion, migration, proliferation and signalling through cytokines, chemokines and other proteins and molecules [14].

- The Endomysium.

The endomysium is the thinner portion of the intramuscular connective tissue

and is directly in contact with and surrounds every single muscle fibre forming its immediate external environment and extends to the perimysium collagen. It is composed of collagen fibre types III, IV and V, and a few collagen type I. It is flexible and can accommodate to the changing volume of muscle during contractions. The endomysium plays key roles in the muscular system as it separates muscle fibers from one another, allows them to glide against one another during muscle contraction and regulates the metabolic exchange between muscle and the blood [15] to mention a few.

1.1.1.3 Fibroblasts. Fibroblasts are the major cells responsible for the production of collagen, glycoaminoglycans, and proteoglycans, which are major components of the extracellular matrix [16]. Fibroblasts, shown in Figure 1.4 [4], are typically spindle-shaped cells with an oval flat nucleus found in the interstitial spaces of organs [17].

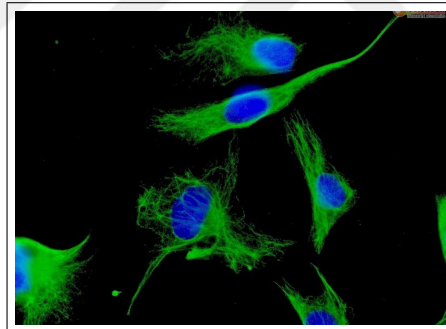


Figure 1.4 Human Cardiac Fibroblasts (CAF) showing the cell body in green and the nucleus in blue. Immunostaining for Vimentin, 600x [4].

The most common function of fibroblasts is to produce collagen and they do so intracellularly by the transcription, translation, and post-translational modification of the collagen mRNA in the nucleus, cytoplasm, and the endoplasmic reticulum (ER) respectively. Finally, the synthesized pro-collagen is moved to the golgi apparatus for final modification before secretion to the extracellular space [18]. The process of collagen production in fibroblasts is regulated by several factors such as the presence of proinflammatory agents, growth factors, mechanical stimulation and ascorbic acid to name a few. For example, it has been reported that collagen synthesis by dermal fibroblasts increased when treated with platelet-derived growth factor (PDGF) and

transforming growth factor-beta (TGF- β) in the presence of ascorbate but inhibited when treated with fibroblast growth factor (FGF) for concentrations greater than 50 ng/ml. [19].

In addition to that, fibroblasts play a very important role in many immune, inflammatory [17],[20],[21], wound healing and repair processes [20],[21]. In fact looking at the wound healing process gives a clear impression about the roles of fibroblasts in such processes. Their function in this process starts when an tissue is injured. The fibroblasts start by proliferating and by chemotaxing to the sites of tissue injury to rebuild the ECM which acts as a scaffold for tissue regeneration. Then these fibroblasts differentiate to myofibroblasts to enable the contraction of the ECM to seal the open wound in case of the loss of tissue [22], [23] as cited in [24]. Fibroblasts also play a role in blood clotting, such as in the production of urokinase plasminogen activators (PAs) and their inhibitors (PAIs). Fibroblasts also express the protease activated receptor PAR1 that enables fibroblasts' responsiveness to activated thrombin [24]. In addition to that, proinflammatory cytokines produced by tissue macrophages activate tissue fibroblasts to produce cytokines, chemokines, prostaglandins (PGE2), and proteolytic enzymes such as metalloproteinases [21] which attract immune cells to the cite of injury.

Fibroblasts can also regulate the behaviour, retention, and survival of the immune cells in damaged tissue and can promote or inhibit the recruitment of circulating leucocytes on endothelial cells via the induction or decrease of cytokine-induced expression of adhesion molecules on endothelial cells [25]. Moreover, although with considerably diminished efficiency relative to professional antigen-presenting cells, fibroblasts have been found to participate in antigen presentation to T Cells [20]. Finally, in addition to the synthesis of proinflammatory cytokines and chemokines and growth factors, there is evidence that fibroblasts can synthesize toll-like receptors (TLRs) and antimicrobial peptides which are all important molecules in the immune response against microorganisms [26].

In fact, the role of fibroblasts in the maintenance of human tissue is so critical that even perturbations in fibroblast function due to persistent activation of the im-

immune system or inflammatory response can ultimately develop into disabling fibrotic disorders [20][25].

1.1.1.4 Chemokines. Chemokines, or chemotactic cytokines [27], are low-molecular-weight proteins that stimulate recruitment of leukocytes or White Blood Cells (WBC). They are secondary pro-inflammatory mediators that are induced by primary pro-inflammatory mediators such as interleukin-1 (IL-1) or tumor necrosis factor (TNF) [28]. Their importance in the skeletal muscle stems from the fact that they are able to induce chemotaxis, or migration of cells, such as fibroblasts, towards the higher concentration of chemokines, to guide cells towards locations of inflammation or disease [29]. About 50 chemokines and 20 chemokine receptors have been discovered [29],[30] and have been attractive targets of therapeutics research studies due to their direct mediation of physiologic and pathologic responses. In the interest of this thesis, four main chemokines were taken into consideration: Platelet-derived growth factor (PDGF), Transforming growth factor-beta ($TGF-\beta$), Interleukin 1 (IL-1) and Insulin-like growth factor 1 (IGF-1).

- **Platelet-derived growth factor (PDGF)**

A family of molecules released from platelets and helps in the wound healing process and the repair of damaged blood vessels [31]. Although originally released from platelets, PDGF is also secreted locally from fibroblasts and leads to fibroblast proliferation and actin filament reorganization which induces a transformation into myofibroblasts, increases the ECM production, inhibits myofibroblast apoptosis and its activity has been linked to pulmonary, hepatic, and renal fibrosis [32].

- **Transforming Growth Factor Beta ($TGF-\beta$)**

Transforming growth factors are a class of cytokines that regulate a variety of functional events including development, differentiation, growth, and immune

responses. Two types of TGF have been reported; alpha and beta, and have been differentiated based on their structure and function [33]. Type alpha TGFs are single chain peptides of 50-53 amino acids cross-linked by three disulphide bonds whereas type beta TGFs have a homodimeric structure comprised of two chains of 112 amino acids, each containing nine cysteine residues and binds to a unique receptor on cell surface. Type alpha usually promotes fibroblast division whereas type beta can stimulate or inhibit the growth of the same cell depending on the condition [33]. Recent work has reported that mammals express three different species of TGF β : TGF β 1, TGF β 2, and TGF β 3 [34]. Finally, it may be important to note that TGF- β 2 is the primary cytokine in human milk and for infants TGF- β is involved in regulating inflammatory responses, establishing oral tolerance by regulatory T cells, inducing IgA production, and enhancing the intestinal epithelial barrier function [35].

- **Interleukin-1 (IL-1)**

Interleukin-1 (IL-1) is the prototypic pro-inflammatory cytokine. There are two forms of IL-1, IL-1 alpha and IL-1 beta and in most studies, their biological activities are indistinguishable. IL-1 affects nearly every cell type, often in concert with another pro-inflammatory cytokine, tumor necrosis factor (TNF). Although IL-1 can upregulate host defenses and function as an immunoadjuvant, IL-1 is a highly inflammatory cytokine [36].

- **The insulin-like growth factors (IGF-I)**

The insulin-like growth factors (IGF-I and IGF-II) play important roles in the regulation of growth and metabolism. While the liver is the main source of circulating IGFs, their production by numerous extrahepatic tissues suggests the existence of autocrine and paracrine modes of action in addition to typical endocrine mechanisms [37]. In the context of skeletal muscle homeostasis, IGF-I is thought to mediate most of the growth-promoting effects of circulating growth hormone (GH) and even also appears to function in a GH-independent autocrine-

paracrine mode in this tissue. Hence, it has been unfortunately an interest to uniformed athletes aiming to gain muscle mass and strength but unaware of its potentially adverse effects which range from disruption of the insulin system to the development of cancer [38].

Finally, it is important to note that in addition to the previously mentioned functions of chemokines, they can also mediate cellular processes such as proliferation, survival, and development depending of the different types of cells [39].

1.2 Skeletal Muscle Pathology And Cerebral Palsy (CP)

In some pathologic conditions, the homeostasis of the skeletal muscle can be altered which can result in abnormal matrix deposition/remodelling, muscle malfunction, muscle loss and, eventually organ failure [40]. Cerebral Palsy is one of those conditions in which muscle function is abnormal and limited due to continuous severe contractures usually very noticeable in the limbs of children at a very young age (few months after birth) and continues to deteriorate up until early adulthood. The disorders in movement and posture are thought to be caused by a nonprogressive lesion of the developing brain [41]. These disorders, usually in the upper or lower extremities, are often accompanied by disturbances of sensation, perception, cognition, communication, and behaviour, and by epilepsy [42].

The feature central to these contractured muscles or spastic muscles is hypertonia (e.g., [43]) and conceivably due to that, spastic muscle tissue is considered typically as stiffened [44]. However, the source of stiffness has long been debated because the use of paralyzing factors such as Botulinum Toxin type-A have not been fully effective suggesting that different causes, in addition to increased stretch reflex activity, contribute to the muscle stiffness. Some researchers have suggested that the stiffness is due to the higher stiffness of the muscles of patients with spasticity while others have suggested the stiffness of the individual muscle fibers of these patients. Additionally, a third opinion suggests that the reason for the muscle stiffness is the shortened muscle fiber state which the muscle adapted to due to the prolonged shortened state due to

the contractures [44].

However, these opinions were mostly rejected by experimentation and opens the possibility that the epimuscular connections of spastic muscle are stiffer [45] or that the prestraining of these structures [46] is increased. Hence, this suggests a bigger role of the myofascial force transmission (MFT) on the mechanical properties of spastic muscle.

1.2.1 Using Botulinum Toxin Type-A in the Treatment of CP

Although CP is a permanent condition, many methods such as surgery and physical therapy have been approached to cure or at least alleviate the accompanying symptoms. However, in 1993 a publication by Koman et al., [47] first announced the usage of Botulinum toxin type A (BTX-A) injections in children with CP to manage the symptoms. Soon after, in 1994, Graham et al.,[48] published the usage of the same approach in the UK. Since then the use of BTX-A has become a 'standard of care' for children with CP in many countries leading to widespread clinical use and the publication and dissemination of consensus statements [42]. Yet, other reports have reported no effective result of using BTX-A in CP management which possibly lead Friedman et al. [49] to state that the source of controversy is partly due to the use of distinct assessment tools and outcome measures as well as the diversity in clinical approaches, cointerventions, and subjects' characteristics. The aims of the treatment are to increase the joint range of motion [50],[51],[52] and to decrease the passive resistance of the muscle at the joint [53]. Hence, BTX-A's mechanism of paralysis is to induce chemo-denervation by prohibiting the release of acetylcholine into the presynaptic cleft at the neuromuscular junction (e.g. [54]) as shown in Figure 1.5.

Accordingly, a characteristic of the BTX-A treatment is decreased muscle force and muscle hyperactivity [55].Albeit these benefits, other papers have reported changes in the structure and properties of the injected muscle such as an increased connective tissue content,[10],[6] decrease in muscle mass and fatty infiltrations[10]. Moreover, in

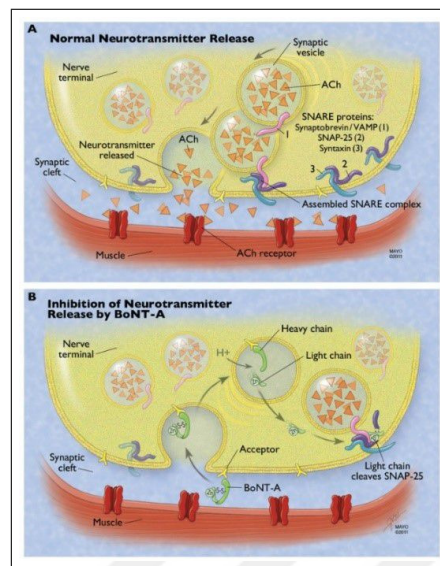


Figure 1.5 BTX-A blocking of Acetylcholine (ACh) at the presynaptic cleft at the neuromuscular junction [5].

a recent animal study by Ateş and Yücesoy [6] it was shown that that exposure to BTX-A causes increased passive force, increased muscle stiffness and collagen content and a decreased length range of force exertion which contradict the treatment aims.

1.2.2 Recent Investigations on BTX-A Effects on Muscle Mechanics.

The study of Ateş and Yücesoy [6] aimed to verify the effects of BTX-A injections on the mechanics of the biarticular synergist of the the tibialis anterior (TA) rat muscle both actively and passively. In the study, the two groups of Wistar rats were separated to control and BTX-A (0.1 U BTX-A) groups. The BTX-A group was injected in the midbelly of the TA and the isometric forces of the extensor digitorum longus (EDL) muscle were measured after proximal and distal lengthening 5 days after injection.

Figure 1.6 below shows an increase in the passive forces of both the EDL and EHL after both proximal and distal lengthening.

In addition to that, the results showed a decrease in the length-force characteristics of the EDL after proximal and distal lengthening as shown in figure 1.7 below. This

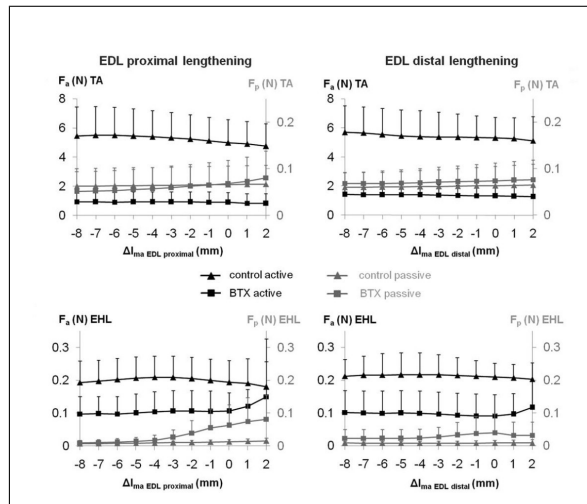


Figure 1.6 An increase in the passive forces of both the EDL and EHL after both proximal and distal lengthening can be seen by looking at the BTX-A passive force markers (grey squares) [6].

can be clearly seen when looking at the decreased length range of BTX-A compared to the control in the figure below.

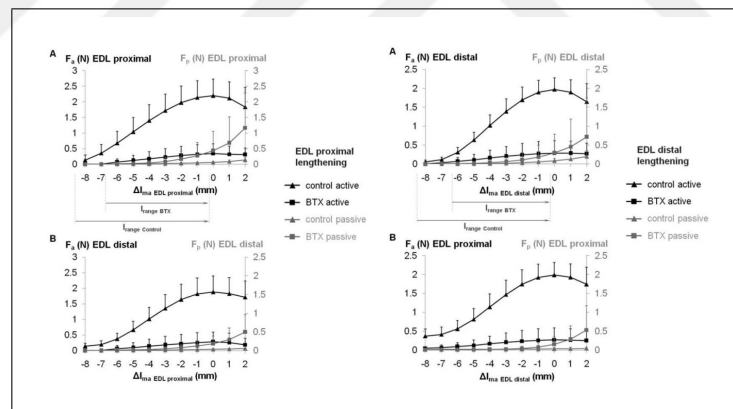


Figure 1.7 An increase in the passive forces of both the EDL and EHL after both proximal and distal lengthening can be seen by looking at the BTX-A passive force markers (grey squares) [6].

These novel BTX-A effects on muscular mechanics could be well attributed to the reported increased collagen content in the injected muscle ECM [6]. Figure 1.8 shows sample histological sections of intramuscular connective tissue staining where the percentage of intramuscular connective tissue content values reported for muscles of the BTX-A group (mean \pm SD: $1.5 \pm 0.6\%$, $6.3 \pm 1.3\%$, and $4.6 \pm 1.2\%$ for the TA, EHL, and EDL, respectively) were significantly higher than those for muscles of the control group ($0.5 \pm 0.2\%$, $3.2 \pm 1.0\%$, and $1.3 \pm 0.5\%$ for the TA, EHL, and EDL,

respectively) [6].

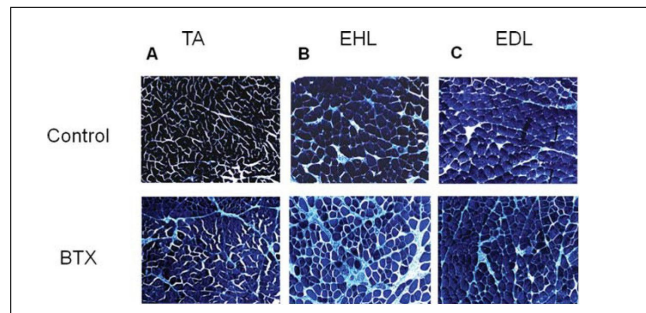


Figure 1.8 Histological samples of the anterior crucial muscle stained for Gomori trichrome for connective tissue. From the left tibialis anterior (TA), extensor hallucis longus (EHL) and extensor digitorum longus (EDL) control (upper) muscles were compared to BTX-A (lower) treated muscles [6].

This collagen increase in the ECM due to BTX-A injections may imply a change in the mechanics of these muscles as suggested by Yücesoy and Huijing [44]. Moreover, an earlier work of Yücesoy et al. [56] suggested that in addition to the supportive role of the ECM in muscle fiber physiology, it also allows the distribution of strain within the fibers and muscle through myofascial force transmission (MFT). This was found by developing a finite element model that models the muscle as two meshes; a muscle fiber mesh, linked elastically to account for the trans-sarcolemmal attachments of the muscle fibers' cytoskeleton and extracellular matrix, with an extracellular matrix mesh; similar to the actual muscle structure.

Moreover, a recent finite element model by Türkoğlu et al. [7] shown in Figure 1.9, proposed that partial paralysis of the muscle due to the BTX-A injections, modelled at different lengths in three cases as shown in Figure 1.10, does not allow the sarcomeres to retract to their original lengths due to lack of activation in the paralyzed muscle. According to the study, this causes the sarcomeres to deform and become longer compared to the BTX-A-Free cases. This "longer sarcomere effect" or LSE, has shown to cause a reduced force reduction capability of the muscle, exclusively originating from the paralyzed muscle, and a shifted muscle optimum length to a lower muscle length. Moreover, LSE in principle is a direct result of the altered muscle fiber-ECM interactions and hence the MFT. Accordingly, any changes within the ECM structure or mechanical properties, will have a noticeable effect on the force production and

structural and mechanical properties of the injected muscle.

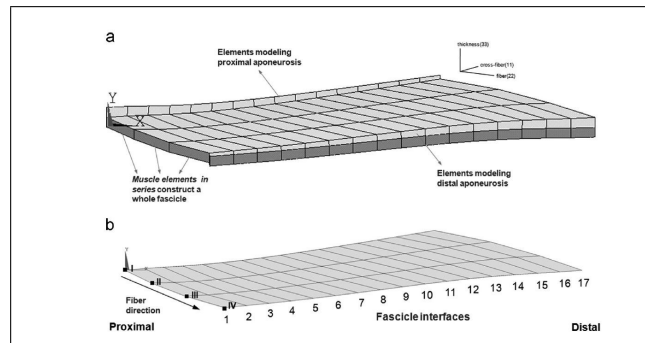


Figure 1.9 The finite element model of the EDL muscle showing three muscle elements in series and seventeen in parallel. Each combination of three muscle elements arranged in series constructs a whole fascicle, seventeen in total. The proximal and distal ends of the muscle elements are connected to elements representing the muscle aponeuroses [7].

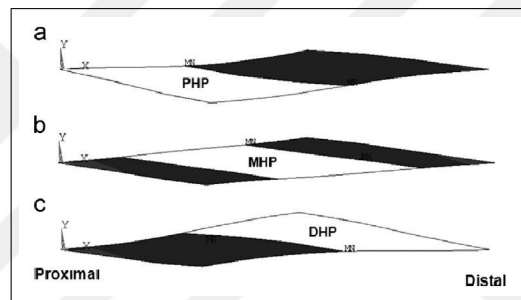


Figure 1.10 Deformed muscle's shape after distal lengthening of BTX-A treated muscle modelled by paralyzing the proximal half (PHP), middle half (MHP), or distal half (DHP) of the muscle.

In addition to that, the model showed that BTX-A muscle fibers showed higher mean fiber direction strains compared to the BTX-A-Free fibers as shown in Figure 1.11.

Furthermore, the reports of an increased passive force of the BTX-A treated muscle [57],[6],[58] motivated Türkoğlu and Yücesoy [59] to utilize the model further to study the effects of BTX-A on muscle mechanics over acute, long-term and post-BTX-A treatment and then compare them to the pre-treatment case. The cases were modelled as the following: pre-treatment case had all the muscle fibers active maximally with no changes on the ECM properties. Acute was modelled as middle-half paralyzed (i.e. MHP) with no changes to the ECM properties. Long-term treatment was modelled with middle-half paralyzed fibers with the ECM properties adapted to BTX-A treatment and finally the post-treatment case was modelled by maximally activating

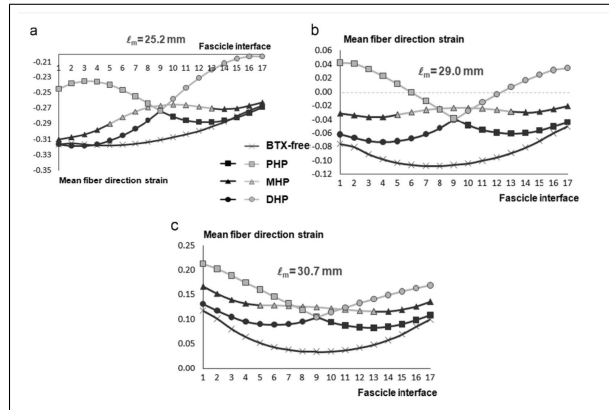


Figure 1.11 The effects of modelling the partial paralysis cases of the BTX-A case on muscle fiber direction mean strain. $\hat{\mu}_m$, or muscle lengths are shown above each figure. The dark plots with the dark bullets indicate the active muscle parts while the grey plots and bullets indicate the paralyzed ones [7].

the muscle fibers and including adapted ECM properties. The results of the model revealed that BTX-A treatment effects are enhanced with the increased ECM stiffness in the long-term and persist post-BTX-A treatment. In addition to that, the LSE is further enhanced in the long term and persists or, for longer muscle lengths, is reversed which leads to a higher force production capacity for the whole muscle post treatment. Additionally, the muscle's optimum length is shifted and is more pronounced in the long-term and in some cases permanently post-treatment. Finally, a narrower length range of force exertion for acute, long-term and post-BTX-A treatment have been also reported.

Hence, modelling BTX-A effects as higher strains compared to the BTX-A-Free case is a logical choice for our modelling purpose in this study which is to model the effects of BTX-A on the muscle fascicles. Moreover, the 30.7mm long muscle fibers had strains which were all positive, so it was chosen as the figure of reference for the ABM model parameters as shown in Figure 1.12.

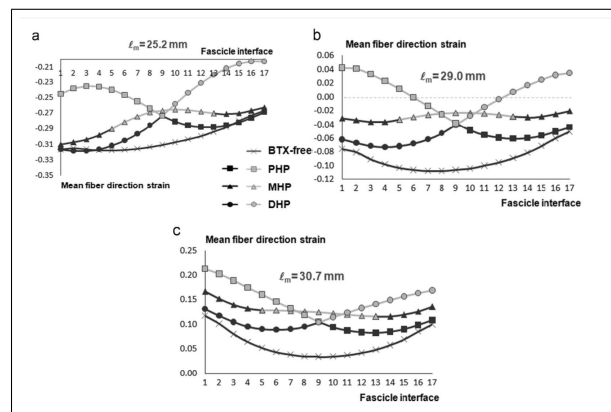


Figure 1.12 Finite element analysis results show increased strain in the BTX-A muscle fiber versus the control muscle fiber [7].

1.3 The Agent-Based Modelling Method

The Agent-based (AB) modelling method is a simulation research technique where components of a process are modelled as "agents" that interact with other agents and their environment or "world" based on a set of rules that govern their interactions. It is a holistic approach where the sum of individual interactions results in an emergent behaviour of the system as a whole. In cases where the interaction between agents is complex and non-linear, AB modelling method has emerged as a powerful tool where the solutions of the differential equations used in the solution of homogeneous systems are insufficient [60] or even do not exist. AB modelling is especially useful in situations where components of a system can be modelled individually to react to their surrounding such as cells within a biological system.

Agent-based modelling has been gaining a lot of popularity especially over the past few years [60]. This modelling method has enabled modellers to investigate characteristics and interactions of even the smallest units within the model under study. Hence, although it has been used mainly in social science and economic studies such as classroom evacuation [8] and the effects of the use of shopbots on market dynamics [61] respectively, agent-based modelling has been used in many fields such as engineering, medicine, and natural sciences to count a few [62]. Hence, agent-based modelling is being used in both the biological and nonbiological fields alike. The Figure 1.13 below

from Liu et al.'s [8] classroom evacuation model shows the typical setup of an agent-based model. Moreover, it is important to note that although the evacuation model used the Netlogo environment, the same components and principles are characteristic of the agent-based modelling method elsewhere. Generally in these models, students, buyers, traders or even organisms would act as the agents, and their surrounding world in which they interact with and with each other would be governed by a set of rules that moderate their interactions.

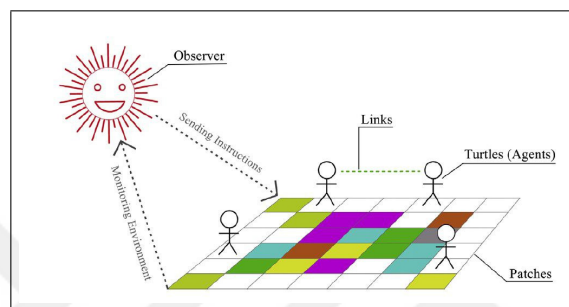


Figure 1.13 The main components of an agent-based model [8].

In addition to that, more recently, the agent-based modelling has gained even more attention in the field of biological sciences. For example, Keshavarzian et al. [63] developed a model for studying arterial growth and remodelling in response to changes in growth factors, proteases, and other signalling factors as well as in blood pressure. The developers defined two super classes of agents for their model; Patches and cells. Patches were 3D components that store ECM, cells, other growth factors which are secreted by the cells and the cells were the main cells in the arterial environment (i.e. endothelial cells (ECs), smooth muscle cells (SMCs) and adventitial fibroblasts (AFs)). The AB model was then coupled with a finite element model to further study the interplay of bio-chemo-mechanical factors in blood vessels and their role in maintaining homeostasis.

Furthermore, more relevant to this thesis, the agent-based modelling was even used in specific branches of biological sciences such muscle biomechanics. For example, Martin [1] developed an agent-based model which aimed to investigate skeletal muscle adaptations in conditions of atrophy and injury and inflammation. The main components of the model were the muscle fibers, fibroblasts, the ECM and chemokines present

in the muscle fibers. In addition to that, the injury and inflammation model was expanded to include inflammatory and satellite stem cells and other inflammatory related factors such as IL-6 and IL-10. Moreover, the model was also used by Martin [1] to design an in vivo experiment of muscle regeneration and by Virgilio et al. [64] to develop a novel multiscale muscle modelling framework to elucidate the relationship between microstructural disease adaptations and modifications in both mechanical properties of muscle and strain in the cell membrane.

Hence, the agent-based modelling method is a very suitable method for studying situations where agent to agent, agent to environment and vice versa interactions can be defined and investigated. In the case of muscle mechanics, this is especially suitable as the muscular system consists of cells, other agents, such as the ECM and its components, and environmental components such as growth factors and other factors which all interact with each other and affect the muscular environment and performance as a whole.

1.4 Goal of the Study

The importance of this study arises from the fact that the mechanical properties and healthy functioning of the muscles are greatly influenced by the composition of the extracellular matrix (ECM). Accordingly, any effects induced by BTX-A injections to this component of the skeletal muscle system is of a potentially prominent importance. The goal of this thesis, hence, is to study how BTX-A affects the injected muscle and its ECM, investigate those effects in the long term and establish the basis for a possible multi-scale model by incorporating the results of the ABM into the previously studied FEM model. Finally, to establish a model that can be used as a possible platform to study therapeutic procedures against CP or to find alternatives to BTX-A.

2. METHODS

2.1 The AB Model

Being very relevant to this thesis, the model developed by Martin [1] was used as a starting point for this investigation. The model includes the necessary parts of a functional muscle system including fibroblasts, muscle fibers, muscular extracellular matrix and the different chemokines such as the growth factors and MMPs. A special advantage of this model to our study is that not only it includes the interactions and components of a skeletal muscle, but it can also be modified to include altered properties of the skeletal muscle such as atrophy. This has been shown to occur as a result of exposure to BTX-A [10],[6],[65].

2.1.1 Components of the AB Model

The model is shown in Figure 2.1. There are four main components that make up the muscular cross section:

1. The muscle fibers
2. The extracellular matrix (ECM)
3. The fibroblasts
4. The chemokines.

It is important to note that the structure of the ABM-generated fascicle has been initialized by setting setup parameters such as the fascicle cross-sectional area, fiber type composition, the number of fibroblasts initially and the number of muscle fibers making up the fascicle.

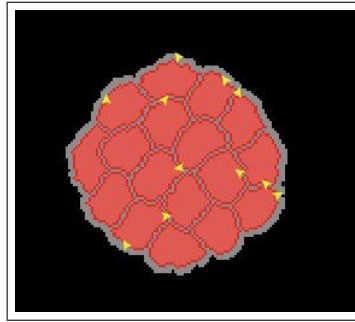


Figure 2.1 The AB generated muscle fascicle cross section showing the main components; muscle fibers (red), ECM (grey), fibroblasts(yellow) and chemokines (not shown). The AB model was developed using the Netlogo 6.0.4 software [9].

- **The muscle fibers (red patches).**

These represent the contractile elements in a real muscular cross section. They are modelled to have properties similar to the physiological muscle: they can be of different fiber types i.e. type I, type IIB, etc and have rules that govern their Insulin-like growth factor 1 (IGF1) secretion and their response to atrophy-based decrease in cross-sectional area.

- **The ECM (grey patches).**

They are the only collagen containing patches within the model and appear in grey. They are the deposits of collagen and chemokines (except for IGF1 which exists in the muscles fibers) in the model and directly affect the behaviour of the fibroblasts. Hence, understanding the ECM-fibroblast interactions has a major importance in this study.

- **The Chemokines.**

They are the growth factors and the matrix metalloproteins (MMPs) which, like in a real muscular environment, guide many biological processes especially collagen deposition by the fibroblasts.

- **The Fibroblasts (yellow arrows).**

They are the main acting agents in the model. They are modelled to migrate, deposit, proliferate, and undergo apoptosis based on a set of physiological rules derived from the literature. Like in a normal muscular structure, fibroblasts are the main producers of collagen, modellers of the ECM and secretors of chemokines. Their behaviour plays a major role in the holistic output of the model. Hence,

correctly modelling their behaviours and interactions is critical to benefiting from the model.

In Türkoğlu et al. [7], BTX-A was shown to cause an increase in strain of the injected muscle i.e. the muscle fibers in a BTX-A treated muscle were shown to be longer. Hence the effects of BTX-A were found to be most appropriately represented as induced strain in the AB model. The model was then utilized by studying three separate cases. In each of the three cases, the results of simulating two fascicles representing the BTX-A and the BTX-A-Free models were compared for four parameters: collagen sum, collagen density, collagen turnover, and fibroblast count.

Collagen sum is the total amount of collagen in the ECM of the modelled fascicle, whereas collagen density and collagen turnover are the amount of collagen within the fascicle divided by the number of patches in the model and the amount of collagen being produced by the fibroblasts during each timestep, respectively. Finally, fibroblast count is the number of fibroblasts available in the fascicle during any given timestep.

The following Figure 2.2 shows the inputs and outputs of the main components of the model.

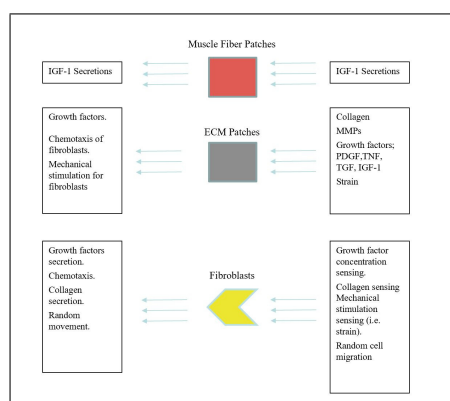


Figure 2.2 The inputs and outputs of the main components of the model.

2.1.2 Equations Governing the Model

The model is based on equations that govern the interactions between the fibroblasts, the chemokines, the muscle fibers and the ECM. These equations are derived from the literature [1]. For example, the movements of the fibroblasts are governed by chemotaxis, or the migration based on the chemokine concentrations around the fibroblasts, the presence of mechanical stimulation [22] and the random movement of cells. These movements are governed by the following algorithms:

```

    if proliferating = 0
  [
  ifelse taxisx = 0
  [
  ifelse taxisy <0
  [set heading 0]
  [set heading 180]
  ]
  [
  set heading atan taxisx taxisy
  ]
  set P sqrt(taxisx ^ 2 + taxisy ^ 2)
  set t timestep * 60
  set dist floor (sqrt(2 * (speed ^ 2) * P * ( t - P * ( 1 - e ^ -1 * t / P )))) / dimension)
  let check random-float (P + stay)
  if check >stay
  :

```

What this short snippet of the code means is that if the fibroblasts are not proliferating and are not taxiing on the x-axis then they set their heading based on the taxis on the y-axis otherwise their heading is set based on the atan of the taxis effects on the x- and the y-axis. Then this taxis affects the persistence to move, p , of the cells and their persistence is also affected by time which both are components of an equation

to determine how much distance they have to move. Finally, their persistence to keep moving or to stay is set based on a random decision based on the p or stay values.

2.2 The Modelled Cases

2.2.1 Case 1 BTX-A Vs. BTX-A-Free

Both the BTX-A and BTX-A-Free had strain induced as random values of strain ranging between 49.5 and 39 for the BTX-A model and between 37.5 and 10.5 for the BTX-A-Free model. These values were obtained from Türkoğlu et al. [7] and modified to strain values reasonable for the model i.e. in the model a constant 5 % strain is equal to approximately 15 units of strain. Hence, for example a 16.5 % BTX-A strain retrieved from figure 12 above would equal 49.5 units of strain in the AB model. The strain was induced in all patches of the model. This means that wherever the fibroblasts migrate to, they will experience strain. The aim of this case was to understand the effects of the different strains on the collagen deposition and fibroblast activity of the modelled fascicles. Figure 2.3 shows the application of strain of the BTX-A and BTX-A-Free cases.

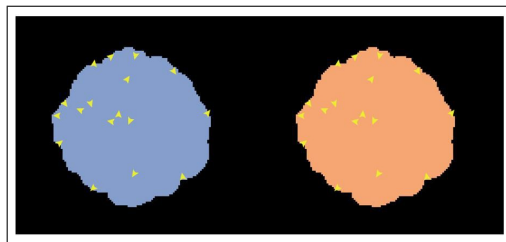


Figure 2.3 The left fascicle shows the patches where the BTX-A strain was applied whereas the right fascicle shows where the BTX-A-Free strain was applied.

2.2.2 Case 2 MHP Vs. BTX-A-Free

The fascicle was modelled based on the middle half paralyzed case (MHP) from Türkoğlu et al.[7] i.e. only half of the fascicle patches were modelled with BTX-A

strains whereas the other half was modelled with BTX-A-Free strains. The aim of this study was to model the fascicle to be closer to the actual in vivo situation and evaluate the results obtained previously from the MHP case of Türkoğlu et al. [7]. Figure 2.4 shows the fascicle of this case.

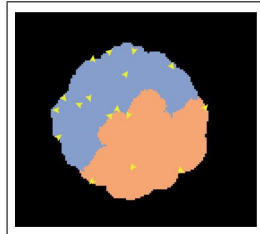


Figure 2.4 The left fascicle shows the patches where the BTX-A strain was applied whereas the right fascicle shows where the BTX-A-Free strain was applied.

2.2.3 Case 3 BTX-A-Free Vs. Physiological MHP

The fascicle in this case was modelled based on MHP fascicle from Türkoğlu et al. [7] however, this time the decaying effects of BTX-A and atrophy were introduced. This is due to the fact that BTX-A has been found to cause paralysis for about 7 days [66] and about 10-15% atrophy in the injected muscle [6]. Hence, the decaying effects of BTX-A and atrophy were modelled accordingly. It is important to note that BTX-A induced strain was modelled to decay within 7 days while atrophy was modelled to gradually decay within 10 days of the injection. The aim of modelling this case was to see the effects of the temporary effects of BTX-A after the injection and how they affect the muscle in the modelled period (approx. 45 days).

2.3 Modelling Procedures

The atrophy model was studied thoroughly to understand how it runs and what were the main effectors in the model. Then, the cases were modelled by changing the strain of the patches and giving each patch a random strain within a range (retrieved from Türkoğlu et al. [7]) depending on its model i.e. BTX-A or BTX-A-Free. For the

second and third case the MHP was modelled by applying BTX-A strain to half of the fibers while keeping the other half strained with normal BTX-A-Free strain. In the third case, the decaying effects of strain and atrophy were modelled by simply applying the half-life equation hence the effects decay with each passing hour.

2.4 Simulation Settings

Both the fascicles of each case were run for 1000 hours (approx. 45 days). In addition to that, the minimum number of runs that would cause a constant average in the measured parameters was found to be about 50 runs as shown in Figure 2.5. However, to avoid any variations from random nature of the model, the model was run for 100 replications.

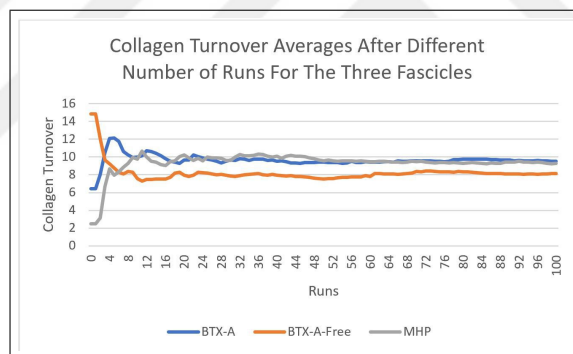


Figure 2.5 Graph showing the averages of collagen turnover and the gradual stabilization after approximately 50 runs for the three fascicles with different strain conditions.

2.5 Processing of Data and Statistics

After obtaining results for each of the 100 runs for each of the three cases, the average of the 100 runs for each parameter was found at each time step resulting in 1000 points for each parameter (from 0 to 999 hours). Then to avoid any statistical issues regarding significance due the large number of data points, the 1000 points were reduced to 99 points by taking the average of each 10 points i.e. batching. The points were then rounded up to the nearest two decimal places to simplify the output and the

significance was measured using the One-way Analysis of Variance (ANOVA) statistical method.



3. RESULTS

The following graphs show the results of the agent-based model simulations for each of the four measured parameters for each of the three cases.

3.1 Case 1: BTX-A Vs. BTX-A-Free

For the first case, the measured parameters were generally higher for the BTX-A case compared to the BTX-A-Free case. For example, the collagen sum and collagen turnover showed approximately a 33% and a 10% increase respectively for the BTX-A case compared to the BTX-A-Free case. However, only the collagen sum and turnover were significant with p-values of 0.000086 and 0.00295 respectively ($p < 0.05$). Figure 3.1 shows the results of the case.

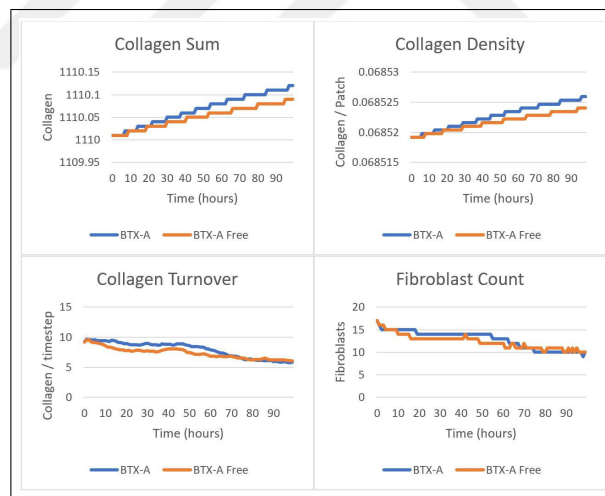


Figure 3.1 The collagen sum, collagen density, collagen turnover and fibroblast count for the fascicle of case 1.

3.2 Case 2: MHP Vs. BTX-A-Free

For the second case, the collagen sum and density showed approximately a 33% increase for the MHP case compared to the BTX-A-Free case whereas, although higher

for the MHP initially, collagen turnover and fibroblast count were higher for the BTX-A-Free model for the majority of the time. Moreover, only the results for the collagen sum and fibroblast count showed significance with p-values of 0.000098 and 0.026283 ($p < 0.05$) whereas the collagen density and collagen turnover did not. Figure 3.2 below shows the results of the case.

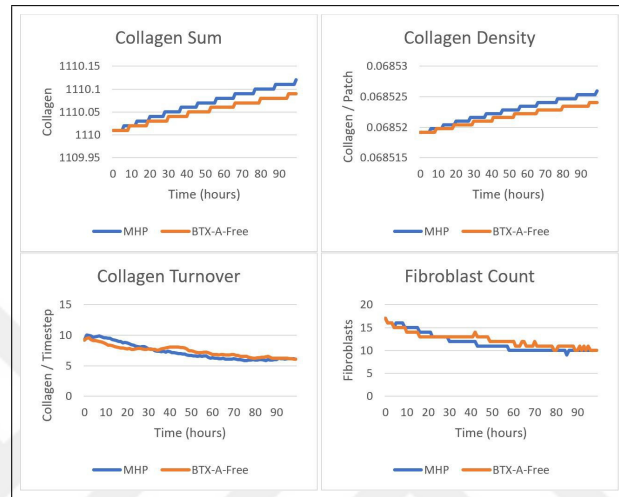


Figure 3.2 The collagen sum, collagen density, collagen turnover and fibroblast count for the fascicle of case 2.

3.3 Case 3: BTX-A-Free Vs. Physiological MHP

Figure 3.3 shows the results of case 3. The collagen sum and density were approximately 20.3 % higher for the physiological MHP model compared to the BTX-A-Free model whereas the collagen turnover and fibroblast count were much higher for the BTX-A-Free model. For this case, all compared parameters were significant with p-values < 0.00001 ($P < 0.05$).

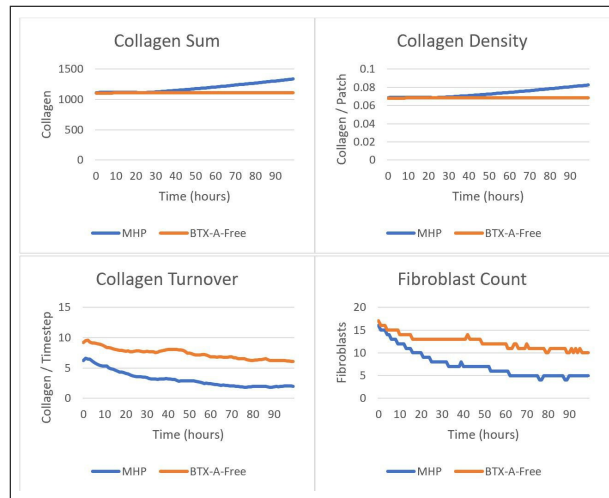


Figure 3.3 The collagen sum, collagen density, collagen turnover and fibroblast count for the fascicle of case 3.

3.4 Validation

In order to validate the results of the model, some parameters were modified to be unrealistically higher than normal in order to see how the model reacts to such changes. In the following example, the BTX-A strain was multiplied by a factor of 100 and the results are shown in Figure 3.4.

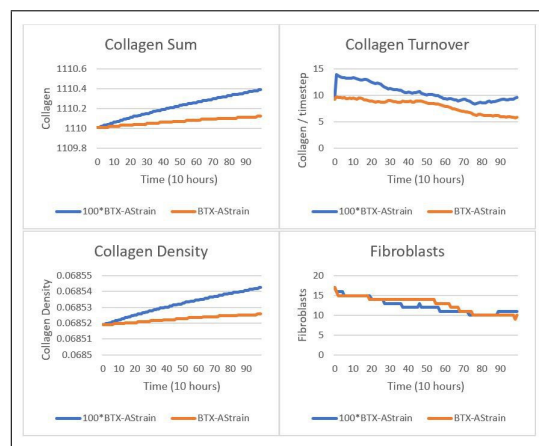


Figure 3.4 The effects of multiplying the BTX-A strain by a factor of 100 on the collagen sum, collagen density, collagen turnover and fibroblast activity.

It is important to note that the collagen sum in the multiplied BTX-A strain fascicle was more than 200% higher than the BTX-A fascicle. The results also showed that the collagen turnover in the muscle ECM also increases significantly. However, the

fibroblasts activity, count to be specific, was not exaggerated by the strain increase, on the contrary it showed higher fibroblasts count for the normal BTX-A strain. Regardless of the reality of the results compared to those in a real muscle fascicle, the model did not crash or fail to produce comparable results due to the unrealistic strain increase parameters.



4. DISCUSSION

In addition to the obtained results, this study has highlighted the ability of the agent-based modelling method in outputting very useful data that can be used in investigating biological research questions especially muscle mechanics. This is mainly because the method allowed investigating at the smallest level and allowed for a stochastic behaviour to emerge based on individual interactions between the different elements of the model. This method also gave more control over the experimental parameters and outcomes such as quickly changing boundary conditions, including or excluding factors, tracking individual parameters and most importantly, the ability to track emergent behaviours of individual units or "agents" at any time of the simulation. However, despite these advantages, there were some challenges regarding this approach. First, dealing with the stochastic nature, random and highly varied nature of the agent-based modelling method was probably the biggest challenge in this study. This was, however, managed by running the model multiple times and averaging the results to get some form of reproducible results. This method of overcoming this challenge was utilized by an arterial adaptation model [67] and a vascular adaptation model [68] where the average of 100 and 15 runs were used respectively. Moreover, it is important to note that although powerful workstations were used, the simulations took a significant amount of time to complete i.e. approximately 6-10 hours per 100 simulations which meant that changing a parameter meant 6-10 hours of computational time. Nevertheless, the agent-based modelling helped to confirm the hypothesis that increased collagen content is correlated with botulinum toxin effects, which was represented in the model as strain characterizing stretch based on earlier finite element modeling.

In order to investigate all aspects of the model, this study was conducted through three cases. The first case involved both BTX-A and BTX-A-Free fascicles modelled with strains representing higher strains for the BTX-A case and lower strains for the BTX-A-Free case as retrieved from Türkoğlu et al. [7]. The aim of this case was to contrast the effects of BTX-A and BTX-A-Free strains on the muscle fascicle. In this

case, only the collagen sum and turnover showed significant increases for the BTX-A fascicles and an increased chemokine levels throughout the simulation time. Therefore, case 1 showed that increased strain causes an increase in fibroblast activity and hence an increase in the deposition of collagen and chemokines which aligns with previous reports in the literature [69],[70],[71].

In the second case the same fascicle was utilized however this time with half of the muscle fascicle modelled with BTX-A strain whereas the other half had BTX-A-Free strain modelled similarly representing the MHP case of Türkoğlu et al.[7]. The aim of this case was to apply BTX-A strains only to the perceived to be injected site hence mimicking the actual condition of the BTX-A injection which usually does not paralyze all fibers of the muscle. The results of this case showed a significant increase for only the collagen sum and fibroblast count for the BTX-A case and that applying BTX-A effects to half of the fascicle gave similar results to the full BTX-A fascicle modelled in case 1 in terms of collagen increase. However, this case also showed that fibroblast activity was not the same very likely due to the random behavior of the fibroblasts modelled or the chemokines behaviors.

Finally, in the third case, atrophy and the decaying BTX-A effects were introduced to the model in order to mimic in vivo conditions as closely as possible. The MHP case was used and compared to the BTX-A-Free model and atrophy was modelled to cause 10-15% atrophy and degrade with time representing the degrading effects of BTX-A overtime after injection. All parameters measured for this case were significant for this case with a significant increase in collagen for the BTX-A model (approx. 20.3%) compared to the BTX-A-Free model. However, what was interesting was the significant increase in fibroblast turnover and count for the BTX-A-Free compared to the BTX-A case. This can be associated to the decaying effects of BTX-A overtime and hence the continuously strained BTX-A-Free muscle would have more strain and hence fibroblast activity compared to the BTX-A muscle.

The importance of the third case rises from the fact that besides the expected increase of collagen content in the muscle ECM due to the BTX-A induced strain,

BTX-A-induced atrophy may also play a significant role in the collagen increase. The third case revealed that even the decaying effects of BTX-A that occur after the initial injection minimize after only 10 days of the injection, they cause more collagen increase than simulating the fascicles for approximately 45 days under BTX-A strains alone. BTX-A induced atrophy was reported by Ateş and Yücesoy[6] and Salari et al. [65] in the injected muscle, and possibly also in the contralateral muscle as reported by Fortuna et al. [10]. In addition to that, atrophy in general has been reported to enhance collagen content in the muscle as reported by Sun et al. [72] and Miller et al. [73]. In fact, the collagen deposited due to atrophy can become severely pathologic and eventually develop fibrosis [72]. This BTX-A induced atrophy may be due to the discrete immobilization caused by the spaced-out injection sessions of BTX-A which, according to Sun et al. [72], is more likely to cause atrophy rather than continuous age or pathology related immobilization. It is important not to neglect that chronic BTX-A injections can trigger an inflammatory response in the injected muscle either due to recurring muscle damage or due to foreign body or substance introduction which could even develop into some form of fibrosis in severe cases [74],[40],[75].

Moreover, it is important to note that the findings of Fortuna et al. [10] are of significant importance because they show that after 3 months of the BTX-A injection, a fatty infiltration becomes obvious in the injected muscle whereas a more enhanced connective tissue appears in the contralateral muscle.

A histological comparison between the BTX-A and control injected and contralateral muscles is shown in Figure 4.1. These findings align with reports of Hamrick et al. [76] who report that fatty infiltration may accompany disuse which also is a major trigger for atrophy.

Finally, it is important to mention that the study had its limitations such as the limited factors measured as it is known that the muscle structure contains many more components that play important roles in the adaptation due to BTX-A injections such as inflammatory agents and satellite stem cells as well as other components of the ECM and collagen types and fiber alignment . Also it is worth mentioning that the model

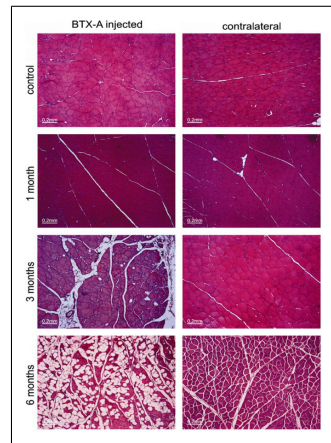


Figure 4.1 Histological comparison between the control BTX-A injected and contralateral muscles after 1, 3, and 6 months of BTX-A injection [10].

did not include special muscle properties that may be characteristic of spastic muscle such as stiffer muscle fibers for example. In addition to that, the agent-based modelling method is a discrete method where events happen after each time step where in reality the nature of biological functions is continuous which may produce some difference in the model outputs.

5. CONCLUSION

To conclude, the model provided valuable information regarding the interactions and possible mechanisms of muscle adaptation due to BTX-A injection. The results of the ABM showed that the BTX-A induced strains cause the most increase in collagen content and fibroblast activity of the muscle, compared to other factors un-negligible such as atrophy which also cause a significant increase in the collagen content of muscle ECM. In addition to that, the model provides first steps into modelling the effects of BTX-A and maybe even modelling of spastic muscle which can be later used as a platform for further understanding CP and perhaps finding better therapeutic protocols for using BTX-A or finding other alternatives.

REFERENCES

1. Martin, K., *Agent-Based Modeling of Skeletal Muscle Adaptation (PhD)*. PhD thesis, University of Virginia, Charlottesville, Virginia, 2015.
2. Krans, J. L., “The sliding filament theory of muscle contraction,” *Nature Education*, Vol. 3, no. 9, p. 66, 2010.
3. Learning, L., *Sliding Filament Model of Contraction | Biology for Majors II*, Portland, OR: Lumen Learning, Undated. Available: <https://courses.lumenlearning.com/wm-biology2/chapter/sliding-filament-model-of-contraction/>.
4. Online, S., *Human Cardiac Fibroblasts*, Carlsbad, CA: Sciencell Online, Undated. Available: <https://www.sciencellonline.com/human-cardiac-fibroblasts.html>.
5. Robertson, C., and I. Garza, “Critical analysis of the use of onabotulinumtoxin (botulinum toxin type a) in migraine,” *Neuropsychiatric Disease and Treatment*, Vol. 35, 2012.
6. Ates, F., and C. Yucesoy, “Effects of botulinum toxin type a on non-injected bi-articular muscle include a narrower length range of force exertion and increased passive force,” *Muscle Nerve*, Vol. 49, no. 6, pp. 866–878, 2014.
7. Turkoglu, A., P. Huijing, and C. Yucesoy, “Mechanical principles of effects of botulinum toxin on muscle length-force characteristics: An assessment by finite element modeling,” *Journal of Biomechanics*, 2014.
8. Liu, R., D. Jiang, and L. Shi, “Agent-based simulation of alternative classroom evacuation scenarios,” *Frontiers of Architectural Research*, Vol. 5, no. 1, pp. 111–125, 2016.
9. Wilensky, U., *NetLogo*, Evanston, IL: NetLogo, 1999. Available: <http://ccl.northwestern.edu/netlogo/>.
10. Fortuna, R., M. Vaz, A. Youssef, D. Longino, and W. Herzog, “Changes in contractile properties of muscles receiving repeat injections of botulinum toxin (botox),” *Journal Of Biomechanics*, Vol. 44, no. 1, pp. 39–44, 2011.
11. Mentis, G., “The spinal and peripheral motor system,” *Fundamental Neuroscience*, pp. 613–630, 2013.
12. Squire, J. M., “Muscle contraction: Sliding filament history, sarcomere dynamics and the two huxleys,” *Global Cardiology Science and Practice*, Vol. 2016, no. 2, 2016.
13. Binder, M., N. Hirokawa, and U. Windhorst, *Encyclopedia of Neuroscience*, Berlin: Springer, 2009.
14. Theocharis, A., S. Skandalis, C. Gialeli, and N. Karamanos, “Extracellular matrix structure,” *Advanced Drug Delivery Reviews*, Vol. 97, pp. 4–27, 2016.
15. Stecco, C., W. Hammer, A. Vleeming, and R. D. Caro, “Deep fasciae,” in *Functional Atlas of the Human Fascial System*, pp. 51–102, London, England: Churchill Livingstone, 2015.
16. Le, A., and J. Brown, “Wound healing,” *Current Therapy in Oral and Maxillofacial Surgery*, pp. 6–10, 2012.

17. Murray, L., D. Knight, and G. Laurent, "Fibroblasts," *Asthma and COPD*, pp. 193–200, 2009.
18. Wu, M., and J. Crane, *Biochemistry and Collagen Synthesis*, Bethesda, MD: NCBI, 2019. Available: <https://www.ncbi.nlm.nih.gov/books/NBK507709/>.
19. Geesin, J., L. Hendricks, J. Gordon, and R. Berg, "Modulation of collagen synthesis by growth factors: The role of ascorbate-stimulated lipid peroxidation," *Archives of Biochemistry and Biophysics*, Vol. 289, no. 1, pp. 6–11, 1991.
20. Williams, I., "Fibroblasts," *Encyclopedia of Immunology*, pp. 905–909, 1998.
21. Gattorno, M., and A. Martini, *Textbook Of Pediatric Rheumatology*, 2011.
22. Gabbiani, G., "The myofibroblast in wound healing and fibrocontractive diseases," *The Journal of Pathology*, Vol. 200, no. 4, pp. 500–503, 2003.
23. Midwood, K. S., L. Williams, and J. E. Schwarzbauer, "Tissue repair and the dynamics of the extracellular matrix," *The International Journal of Biochemistry Cell Biology*, Vol. 36, no. 6, pp. 1031–1037, 2004.
24. Kendall, R., and C. Feghali-Bostwick, "Fibroblasts in fibrosis: Novel roles and mediators," *Frontiers in Pharmacology*, Vol. 5, 2014.
25. Linthout, S. V., K. Miteva, and C. Tschöpe, "Crosstalk between fibroblasts and inflammatory cells," *Cardiovascular Research*, Vol. 102, no. 2, pp. 258–269, 2014.
26. Bautista-Hernandez, L., J. Gomez-Olivares, B. Buentello-Volante, and V. B. de Lucio, "Fibroblasts: The unknown sentinels eliciting immune responses against microorganisms," *European journal of microbiology immunology*, Vol. 7, no. 3, pp. 151–157, 2017.
27. Burbach, J., "Mammalian neuropeptide families," *Encyclopedia Of Neuroscience*, pp. 635–648, 2009.
28. Groves, D., and Y. Jiang, "Chemokines, a family of chemotactic cytokines," *Critical Reviews in Oral Biology Medicine*, Vol. 6, no. 2, pp. 109–118, 1995.
29. Wedemeyer, M., B. Mueller, B. Bender, J. Meiler, and B. Volkman, "Modeling the complete chemokine-receptor interaction," *Methods in Cell Biology*, pp. 289–314, 2019.
30. Gravallesse, E. M., and P. A. Monach, "The rheumatoid joint: Synovitis and tissue destruction," *Rheumatology: Sixth Edition*, pp. 768–784, 2014.
31. Institute, N. C., *NCI Dictionary of Cancer Terms*, Bethesda, MD: National Cancer Institute, Undated. Available: <https://www.cancer.gov/publications/dictionaries/cancer-terms/def/platelet-derived-growth-factor>.
32. Kwan, P., A. Desmouliere, and E. Tredget, "Molecular and cellular basis of hypertrophic scarring," *Total Burn Care*, Vol. 5, pp. 495–505, 2012.
33. Roberts, A. B., and M. B. Sporn, "Transforming growth factors," *Cancer Surveys*, Vol. 4, no. 4, pp. 683–705, 1985.
34. Sollome, J., and R. Fry, "Environmental contaminants and the immune system: A perspective systems," in *Systems Biology in Toxicology and Environmental Health*, pp. 171–186, Cambridge, MA: Academic Press, 2015.

35. Dupont, T., "Donor milk compared with mother's own milk," *Hematology, Immunology and Infectious Disease: Neonatology Questions and Controversies*, Vol. 43, 2018.
36. Dinarello, C., "Interleukin-1," *Cytokine Growth Factor Reviews*, Vol. 8, no. 4, pp. 253–265, 1997.
37. LeRoith, D., M. McGuinness, J. Shemer, B. Stannard, F. Lanau, T. Faria, *et al.*, "Insulin-like growth factors," *Neurosignals*, Vol. 1, no. 4, pp. 173–181, 1992.
38. Adams, G., "Insulin-like growth factor in muscle growth and its potential abuse by athletes," *Western Journal of Medicine*, Vol. 175, no. 1, pp. 7–9, 2001.
39. Wang, X., J. Sharp, T. Handel, and J. Prestegard, "Chemokine oligomerization in cell signaling and migration," *Progress in Molecular Biology and Translational Science*, pp. 531–578, 2013.
40. Bersini, S., M. Gilardi, M. Mora, S. Krol, C. Arrigoni, C. Candrian, *et al.*, "Tackling muscle fibrosis: From molecular mechanisms to next generation engineered models to predict drug delivery," *Advanced Drug Delivery Reviews*, Vol. 129, pp. 64–77, 2018.
41. Wiley, S., and N. Lanphear, "Cerebral palsy," *Pediatric Clinical Advisor*, pp. 102–104, 2007.
42. Multani, I., J. Manji, T. Hastings-Ison, A. Khot, and K. Graham, "Botulinum toxin in the management of children with cerebral palsy," *Pediatric Drugs*, pp. 1–21, 2019.
43. Botte, M., V. Nickel, and W. Akeson, "Spasticity and contracture physiologic aspects of formation," *Clinical Orthopaedics and Related Research*, Vol. 233, pp. 7–18, 1988.
44. Yucesoy, C., and P. Huijing, "Substantial effects of epimuscular myofascial force transmission on muscular mechanics have major implications on spastic muscle and remedial surgery," *Journal of Electromyography and Kinesiology*, Vol. 17, no. 6, pp. 664–679, 2007.
45. Smeulders, M. J. C., *Introducing intraoperative direct measurement of muscle force and myofascial force transmission in tendon transfer for cerebral palsy*. PhD thesis, University of Amsterdam, Amsterdam, The Netherlands, 2004.
46. Yucesoy, C., G. Baan, B. Koopman, H. Grootenboer, and P. Huijing, "Pre-strained epimuscular connections cause muscular myofascial force transmission to affect properties of synergistic ehl and edl muscles of the rat," *Journal of Biomechanical Engineering*, Vol. 127, no. 5, pp. 819–828, 2005.
47. Koman, L., J. Mooney, B. Smith, A. Goodman, and T. Mulvaney, "Management of cerebral palsy with botulinum-a toxin," *Journal Of Pediatric Orthopaedics*, Vol. 13, no. 4, pp. 489–495, 1993.
48. Cosgrove, A., I. Corry, and H. Graham, "Botolinum toxin in the managment of the lower limb in cerebral palsy," *Developmental Medicine Child Neurology*, Vol. 36, no. 5, pp. 386–396, 1994.
49. Friedman, B., and R. Goldman, "Use of botulinum toxin a in management of children with cerebral palsy," *Canadian Family Physician Medecin de Famille Canadien*, Vol. 57, no. 9, pp. 1006–1073, 2011.

50. Koman, L., J. Mooney, B. Smith, F. Walker, and J. Leon, "Botulinum toxin type a neuromuscular blockade in the treatment of lower extremity spasticity in cerebral palsy: A randomized, double-blind, placebo-controlled trial," *Journal of Pediatric Orthopaedics*, Vol. 20, no. 1, pp. 108–115, 2000.
51. Sutherland, D., K. Kaufman, M. Wyatt, H. Chambers, and S. Mubarak, "Double-blind study of botulinum a toxin injections into the gastrocnemius muscle in patients with cerebral palsy," *Gait Posture*, Vol. 10, no. 1, pp. 1–9, 1999.
52. Wong, V., "Use of botulinum toxin injection in 17 children with spastic cerebral palsy," *Pediatric Neurology*, Vol. 18, no. 2, pp. 124–131, 1998.
53. Sheean, G., "Botulinum treatment of spasticity: Why is it so difficult to show a functional benefit?," *Current Opinion in Neurology*, Vol. 14, no. 6, pp. 771–776, 2001.
54. Brin, M., "Botulinum toxin: Chemistry, pharmacology, toxicity, and immunology," *Muscle Nerve*, Vol. 20, pp. 146–168, 1997.
55. Ates, F., and C. Yucesoy, "Botulinum toxin type-a affects mechanics of non-injected antagonistic rat muscles," *Journal Of The Mechanical Behavior Of Biomedical Materials*, Vol. 84, pp. 208–216, 2018.
56. Yucesoy, C., B. Koopman, P. Huijing, and H. Grootenboer, "Three-dimensional finite element modeling of skeletal muscle using a two-domain approach: linked fiber-matrix mesh model," *Journal of Biomechanics*, Vol. 35, no. 9, pp. 1253–1262, 2002.
57. Yucesoy, C., and E. Arikan, "Btx-a administration to the target muscle affects forces of all muscles within an intact compartment and epimuscular myofascial force transmission," *Journal of Biomechanical Engineering*, Vol. 134, no. 11, 2012.
58. Yucesoy, C., A. Turkoglu, S. Umur, and F. Ates, "Intact muscle compartment exposed to botulinum toxin type a shows compromised intermuscular mechanical interaction," *Muscle Nerve*, Vol. 51, no. 1, pp. 106–116, 2014.
59. Turkoglu, A., and C. Yucesoy, "Simulation of effects of botulinum toxin on muscular mechanics in time course of treatment based on adverse extracellular matrix adaptations," *Journal of Biomechanics*, Vol. 49, no. 7, pp. 1192–1198, 2016.
60. Bonabeau, E., "Agent-based modeling: methods and techniques for simulating human systems," *Proceedings Of The National Academy Of Sciences*, Vol. 99, pp. 7280–7287, 2002.
61. Kephart, J., J. Hanson, and A. Greenwald, "Dynamic pricing by software agents," *Computer Networks*, Vol. 32, no. 6, pp. 731–752, 2000.
62. Macal, C., and M. North, "Introductory tutorial: Agent-based modeling and simulation," *Proceedings of the Winter Simulation Conference 2014*, 2014.
63. Keshavarzian, M., C. A. Meyer, and H. N. Hayenga, "Mechanobiological model of arterial growth and remodeling," *Biomechanics and Modeling in Mechanobiology*, Vol. 17, no. 1, pp. 87–101, 2018.
64. Virgilio, K. M., K. S. Martin, S. M. Peirce, and S. S. Blemker, "Multiscale models of skeletal muscle reveal the complex effects of muscular dystrophy on tissue mechanics and damage susceptibility," *Interface Focus*, Vol. 5, no. 2, p. 20140080, 2015.

65. Salari, M., S. Sharma, and M. Jog, "Botulinum toxin induced atrophy: An uncharted territory," *Toxins*, Vol. 10, no. 8, p. 313, 2018.
66. Schantz, E., and E. Johnson, "Properties and use of botulinum toxin and other microbial neurotoxins in medicine," *Microbiological Reviews*, Vol. 56, no. 1, pp. 80–99, 1992.
67. Thorne, B. C., H. N. Hayenga, J. D. Humphrey, and S. M. Peirce, "Toward a multi-scale computational model of arterial adaptation in hypertension: Verification of a multi-cell agent based model," *Frontiers in Physiology*, Vol. 2, 2011.
68. Garbey, M., S. Casarin, and S. A. Berceci, "Vascular adaptation: Pattern formation and cross validation between an agent based model and a dynamical system," *Journal of Theoretical Biology*, Vol. 429, pp. 149–163, 2017.
69. Hara, M., T. Fujii, R. Hashizume, and Y. Nomura, "Effect of strain on human dermal fibroblasts in a three-dimensional collagen sponge," *Cytotechnology*, Vol. 66, no. 5, pp. 723–728, 2013.
70. H. J. Kim, H. Kim, M. P. Lewis, and I. Wall, "Impact of mechanical stretch on the cell behaviors of bone and surrounding tissues," *Journal of Tissue Engineering*, Vol. 7, 2016.
71. Manuyakorn, W., D. E. Smart, A. Noto, F. Bucchieri, H. Haitchi, S. T. Holgate, P. H. Howarth, and D. E. Davies, "Mechanical strain causes adaptive change in bronchial fibroblasts enhancing profibrotic and inflammatory responses," *PLoS ONE*, Vol. 11, no. 4, p. e0153926, 2016.
72. Sun, S., K. Henriksen, M. A. Karsdal, I. Byrjalsen, J. Rittweger, *et al.*, "Collagen type iii and vi turnover in response to long-term immobilization," *PLoS ONE*, Vol. 10, p. 12, 2015.
73. Miller, T., L. Lesniewski, J. Muller-Delp, A. Majors, D. Scalise, and M. Delp, "Hindlimb unloading induces a collagen isoform shift in the soleus muscle of the rat," *American Journal of Physiology-Regulatory, Integrative and Comparative Physiology*, Vol. 281, no. 5, pp. R1710–R1717, 2001.
74. Haneke, E., "Managing complications of fillers: Rare and not-so-rare," *Journal of Cutaneous and Aesthetic Surgery*, Vol. 8, no. 4, pp. 198–210, 2015.
75. Nitecka-Buchta, A., K. Walczynska-Dragon, J. Batko-Kapustecka, and M. Wieckiewicz, "Comparison between collagen and lidocaine intramuscular injections in terms of their efficiency in decreasing myofascial pain within masseter muscles: A randomized, single-blind controlled trial," *Pain Research and Management*, Vol. 2018, pp. 1–10, 2018.
76. Hamrick, M., M. McGee-Lawrence, and D. Frechette, "Fatty infiltration of skeletal muscle: Mechanisms and comparisons with bone marrow adiposity," *Frontiers in Endocrinology*, Vol. 7, 2016.